NASA TN D-208

NASA TN D-208

7N-39
197740

TECHNICAL NOTE
D-208

AN INVESTIGATION OF NONPROPAGATING FATIGUE CRACKS

By Arthur J. McEvily, Jr., and Walter Illg

Langley Research Center
Langley Field, Va.

NATIONAL AERONAUTICS AND SPACE ADMINISTRATION

WASHINGTON December 1959

(NASA-TN-D-208) AN INVESTIGATION OF NONPROPAGATING FATIGUE CRACKS (NASA. Langley Research Center) 32 p

N89-70953

Unclas
00/39 0197740

.Q

NATIONAL AERONAUTICS AND SPACE ADMINISTRATION

TECHNICAL NOTE D-208

AN INVESTIGATION OF NONPROPAGATING FATIGUE CRACKS

By Arthur J. McEvily, Jr., and Walter Illg

SUMMARY

Through consideration of the stresses existing at the tip of a fatigue crack an attempt is made to account for nonpropagating fatigue cracks. It is concluded that such cracks may form under constant-amplitude cyclic loading if the crack closes during compression or if the effective radius of the crack is larger than that of the initial notch. The results of experimental work on steel and aluminum alloys compare favorably with predictions.

INTRODUCTION

A number of investigations (refs. 1 to 9) have established the fact that under certain conditions it is possible for nonpropagating fatigue cracks to develop during constant-amplitude loading. Most of the evidence for this phenomenon has been obtained by sectioning notched specimens after millions of cycles of stress had been applied, but in at least one case (ref. 5) direct experimental evidence has been obtained through observation of the growth of fatigue cracks. A number of explanations for this phenomenon (for example, refs. 5, 10, and 11) have been put forth, but they are either qualitative or not entirely consistent with the published data in this field. In the present paper a brief review and discussion of these explanations is given, and a more quantitative interpretation of the phenomenon is presented and compared with published experimental results for mild steel and two aluminum alloys. In order to check certain predictions concerning nonpropagating fatigue cracks, a number of additional tests were made on the aluminum alloys 2024-T3 and 7075-T6. The results of these tests are also discussed.

SYMBOLS

A,A',B,B',C,C',O,D,E identification symbols on stress-strain curves (see fig. 1)

K_N theoretical stress-concentration factor corrected for size effect

$K_{N,crack}$ size-corrected theoretical stress-concentration factor for a fatigue crack

$K_{N,notch}$ size-corrected theoretical stress-concentration factor for a machined notch

K_T theoretical stress-concentration factor

l total length of crack or internal notch, in.

N number of cycles

R ratio of minimum nominal stress to maximum nominal stress in fatigue cycle

R_e effective stress ratio at tip of stress raiser

S_f fatigue limit, ksi

S_{net} instantaneous net-section stress, ksi

ϵ local strain at tip of fatigue crack, in./in.

ρ radius of curvature, in.

ρ' Neuber material constant, in.

ρ_e effective radius of curvature of tip of fatigue crack, in.

ρ_{crack} radius of curvature of tip of crack

ρ_{notch} radius of curvature of notch

σ local stress at tip of fatigue crack, ksi

L
4
2
9

EFFECTIVENESS OF THE FATIGUE CRACK AS A STRESS RAISER

Preliminary Considerations

In several recent papers (refs. 12 to 14) certain concepts concerning the behavior of fatigue cracks under static or cyclic loading were developed. Inasmuch as it is believed that these same ideas can be extended to account for nonpropagating fatigue cracks, a brief review of the pertinent points will be given.

The approach in these papers has been to consider that fatigue cracks are stress raisers characterized by a length l and an effective tip radius ρ_e. This approach is inherently semiempirical since ρ_e is determined from test data. Once ρ_e is known it is possible to compute the theoretical stress-concentration factor K_T for any combination of specimen width and crack length through an extension of Neuber's (ref. 15) or Howland's (ref. 16) method. The stress-concentration factors are then modified for size effect after the manner of reference 15 and are designated as K_N, where K_N is given by

L
4
2
9

$$K_N = 1 + \frac{K_T - 1}{1 + \sqrt{\frac{\rho'}{\rho_e}}} \tag{1}$$

and where ρ' is a material constant which introduces size effect. Neuber thought of ρ' as the edge dimension of a block of material across which no stress gradient could exist and, therefore, the stress-concentration factor was reduced even in the elastic range. This constant is empirically determined. As an illustration of the influence of the size-effect correction, consider the case of an internal elliptical notch of length l and of tip radius ρ in an infinitely wide sheet loaded in tension in the plane of the sheet, perpendicular to the major axis of the ellipse. For this case equation (1) becomes

$$K_N = 1 + \frac{2\sqrt{\frac{l}{2\rho}}}{1 + \sqrt{\frac{\rho'}{\rho}}}$$

As $\rho \rightarrow 0$ with l fixed, $K_N \rightarrow 1 + 2\sqrt{\frac{l}{2\rho'}}$ which is a constant; or if $l \rightarrow 0$, $K_N \rightarrow 1$. Both of these limits are in accord with experience, namely, that there is a limit to the effectiveness of a notch of decreasing radius, and that extremely small defects are without effect on engineering materials.

Previous work (refs. 12 to 14) indicates that for fatigue cracks ρ_e does not approach zero but is of finite value. Results of tests on aluminum alloys suggest that ρ' and ρ_e are of the same order. With ρ_e taken as equal to ρ', satisfactory correlation of experimental results has been obtained for a wide range of specimen widths and crack lengths, both for tests involving the effect of fatigue cracks on static strength and also for tests involving the rate of propagation of fatigue cracks under cyclic loading. As a result of these experiments, numerical values of ρ_e of 0.002 and 0.003 inch have been assigned to the aluminum alloys 7075-T6 and 2024-T3, respectively. The assignment of these specific values tacitly assumes that stress history is unimportant, a matter which will be discussed in subsequent sections. In addition, by taking ρ' equal to ρ_e, equation (1) is simplified to

$$K_N = 1 + \frac{K_T - 1}{2} \qquad (2)$$

L
4
2
9

The Effective Radius of a Fatigue Crack

Visual examination of fatigue cracks in the aforementioned aluminum alloys indicates that the tip radii are geometrically much smaller than the numerical values stated previously. Some discussion of this matter is presented in this section.

Several effects can play a role in accounting for the rather large numerical value of the effective radius as compared with the geometric value. It is believed that the change in tip radius due to plastic deformation and the development of residual compressive stresses are of major importance in this respect. Other factors such as bifurcation of the crack and meandering out of the plane of maximum tensile stress may also increase the effective radius, but to a lesser extent; the reason is that in the course of the experimental investigation described in references 13 and 14, although both of the aforementioned effects were at times present, they did not appear to affect the rate of fatigue-crack propagation. In addition, Frost and Dugdale (ref. 7) point out that bifurcation is not a necessary condition for the formation of nonpropagating cracks.

In order to illustrate the role of plastic deformation in determining the effective radius, it is assumed, as in reference 13, that fatigue-crack propagation at low nominal stress levels occurs in two stages. During the first stage the material at the tip of the crack is cycled until fracture occurs. During the second stage the fracture advances an incremental amount into the material ahead of the crack and is arrested because of the more ductile nature of the material at the new crack tip. Then, the first-stage process begins again and the sequence is repeated over and over until static fracture of the entire specimen finally occurs. Upon each incremental advance, previous history is essentially eliminated.

In the following discussion it is assumed that one of these advances has just occurred and that the process associated with the first stage is about to begin.

In figure 1 several examples of idealized stress-strain behavior at the tip of a fatigue crack are shown. This figure will be used to help explain the effect of residual stresses on the effective radius. Figure 1(a) illustrates the idealized stress-strain behavior at the tip of a fatigue crack for loading with $R = -1$ at a low nominal stress value. When the crack is first loaded in tension the stress-strain path is between the points labeled O, D, and E (which can be referred to as ODE). Upon unloading, a residual compressive stress corresponding to point B is developed. In subsequent cycles the stress-strain behavior might follow the path BABCB, the stress amplitude being somewhat less than the original amount because of the effect of increase in tip radius as a result of plastic deformation. Within the region of peak stress at the tip of the crack, whose linear dimension would be of the order of ρ', the fatigue process proceeds at critical sites although the average peak stress of the region is within the elastic range. Incidentally, if the first half-cycle were compression, this description would not be altered inasmuch as such loading would merely close the crack and eliminate its effectiveness as a stress raiser during this half-cycle.

Figure 1(b) illustrates the case of loading with $R = -1$ at a higher stress than that in figure 1(a). For this case a greater residual compressive stress would be expected because of the larger plastic strain in tension; because of the greater plastic strain in the first tension half-cycle, the crack would not close as much on unloading as in figure 1(a). In the compression half-cycle, the yield stress would be less than that in the tension half-cycle because of the Bauschinger effect; and as the compression load increased, the stress at the tip would approach point C. Once point C, which lies on the σ-axis, is reached the strain at the tip of the crack is zero. Any further increase in compression load would have little effect on the material at the tip of the crack because stress concentration is eliminated and the net section is increased. For loading to point C the final cyclic path would be along ABC, with A and B being slightly higher than A' and B', respectively, because of the effect of reverse plastic strain on the residual compressive stress B'.

At stress levels higher than those in figure 1(b) it is possible that the tip stress would move along the compression yield stress line on unloading from the initial tension stress and would approach the position of zero strain on the σ-axis as a limit. Figure 1(c) depicts this case. Here, the final cycling is between the points labeled B, C, and A. For this case the compressive half-cycle would have no effect. Consequently, $R = 0$ and $R = -1$ would be equivalent for the same applied load amplitude. In figures 1(a) and 1(b), however, loading with

R = -1 would be more severe than loading with R = 0 because in these cases the compression stress would have an effect.

Incidentally, in this simple explanation, the amount of residual compression stress developed in figure 1(c) is the maximum possible. For real materials this situation would be altered in that the stress-strain curves and Bauschinger effects would probably not be as well behaved as herein considered. However, results indicating the type of behavior as shown in figure 1 have been presented in reference 14. For example, at low stresses for the aluminum alloy 7075-T6, loading with R = -1 was more severe than that with R = 0, but at higher stresses the rate of fatigue-crack propagation was about the same for each type of loading.

L
4
2
9

As stated previously, it is believed that the residual compressive stress is largely responsible for the discrepancy between the geometric radius and effective radius of a fatigue crack, for this stress would reduce the effectiveness of the fatigue crack as a stress raiser. Since the effective radius is empirically determined, the effect of residual stresses is automatically taken into account in determining the macroscopic behavior of parts containing fatigue cracks. However, as seen in figure 1 the magnitude of the residual compressive stress varies with the applied stress and type of loading, which could mean that the effective radius should also vary. However, in previous work (refs. 12 to 14), as an approximation, the effective radius has been considered to be a constant for a given material, and this work will be briefly reviewed in an attempt to resolve this point.

Methods of Determining the Effective Radius

The first evaluation of the effective radius of a fatigue crack was made in tests of the effect of fatigue cracks on the static strength of the aluminum alloys 2024-T3 and 7075-T6 (ref. 12). In these tests fatigue cracks were formed at R = 0 in axially loaded sheet specimens at stresses ranging from 5 to 30 ksi based on the original net section. The specimens were then loaded to failure under tension loading, and from the test results an equivalent radius ρ_e was determined, with the assumption that failure occurred when the stress-concentration factor (modified for size and plasticity effects) multiplied by S_{net} equaled the ultimate tensile strength of the material. (The constant ρ' had already been determined in ref. 12 from static tests to failure of sheet specimens containing notches of known radii.) For such a wide range of fatigue stress levels it might be expected that a corresponding range of residual stresses would have been introduced with concomitant effect on the effective radius. However, in the subsequent static tests to fracture of the specimens, extensive plastic deformation took place at the tip of the cracks. It is believed that this plastic deformation largely eliminated residual stress differences which may have been present. In addition, the cracks usually grew a short distance prior to the point of maximum load, thereby further eliminating the effects of previous test history. It, therefore, appears that the results are not very sensitive to variations in the residual stress state which may have been present at the tips of the cracks. Hence, a single value of ρ_e may justifiably be used in this case, especially in view of the satisfactory correlation which was obtained.

In the reports on the rate of fatigue-crack propagation in the aluminum alloys 2024-T3 and 7075-T6 (refs. 13 and 14), it was considered that at low stress levels the effective principal stress existing at the tip of a fatigue crack was given by $K_N S_{net}$. At both $R = 0$ and $R = -1$ the minimum value of stress S_{net} required to propagate a fatigue crack was determined, and it was assumed that the value of $K_N S_{net}$ at the tip of the crack corresponding to this minimum stress level corresponded to the fatigue limit of unnotched specimens of these materials under the same R ratio. It was found that the value of S_{net} at this minimum stress level was less for loading with $R = -1$ than with $R = 0$. Solving for ρ_e (with the assumption that ρ' equaled ρ_e) led to the same value of ρ_e for both $R = 0$ and $R = -1$. (The fatigue limits for both of these aluminum alloys in the unnotched condition were approximately 20 ksi for $R = -1$ and 30 ksi for $R = 0$.) The fact that at $R = -1$ the cracks grew at values of $K_N S_{net}$ slightly greater than 20 ksi suggested that the cracks were not closed even in compression (corresponding to fig. 1(a)). The fact that at both $R = 0$ and $R = -1$ the same effective radius was obtained for a given material indicates that the state of residual stress was about the same for each type of loading (also corresponding to fig. 1(a)). These tests at low stress levels for the determination of ρ_e should be very sensitive inasmuch as no plasticity factor is involved as was the case in the static tests. It is significant that the results of both types of tests yielded consistent values for ρ_e.

The results of fatigue-crack propagation tests at higher stress levels were plotted as shown in figure 2, and it can be seen that good correlation of crack-propagation rates as a function of $K_N S_{net}$ was obtained. In computing the value of K_N, a constant value of ρ_e was used. However, if there were an increase in residual compressive stress with increase in $K_N S_{net}$ (and corresponding increase in ρ_e), this increase of residual stress would not be apparent from these results. An auxiliary test which will now be briefly described can shed some light on this matter.

A 2024-T3 sheet specimen was subjected to a cyclic loading of ± 40 ksi and a short fatigue crack was grown, so that the resultant value of $K_N S_{net}$ $\left(\rho_e = 0.003 \text{ inch}\right)$ was ± 375 ksi. The applied load was then decreased to ± 6 ksi, or a value of $K_N S_{net}$ of ± 53.7 ksi. At this level no further growth of the crack was detected up to 10^7 cycles at which time the test was terminated. (A "nonpropagating crack" was formed.)

A similar specimen was subjected to a cyclic loading of slightly less than ± 6 ksi so that when the crack grew to the same length as in the aforementioned test, the values of $K_N S_{net}$ $\left(\text{and, of course, } S_{net}\right)$ were the same as those at the lower stress level in the aforementioned test. Further cycling caused further growth of the crack and complete failure of the specimen in 1.6×10^6 cycles.

L
4
2
9

Hence, it is concluded that a much larger residual compression stress had been introduced at the higher stress level, which means that ρ_e is not a constant but actually increases with increasing stress level. However, at constant stress levels or where the stress does not change very much, the rate of fatigue-crack propagation should be as given in figure 2, based on a constant value of ρ_e. Incidentally, had the sequence of stress levels in the high-to-low stress experiment been reversed, it is expected that the rate of propagation at the higher level would have been as shown in figure 2, for the residual stress would have been increased immediately (on the assumption that the material did not tear on application of the higher load). These considerations would also be of importance in any attempt to formulate a theory to account for fatigue-crack propagation under conditions of variable-amplitude loading, but a straightforward summation based on figure 2 should be on the conservative side. Further refinement would require that the variation of ρ_e with stress level be taken into account.

The residual stresses developed at the tip of a crack may also account for a feature of experimental work which is often reported in connection with fatigue-crack-propagation studies, namely, that for centrally notched sheet specimens the two fatigue cracks which are formed are almost of equal length throughout the test. Usually, one crack forms before the other, and thus, the resultant stress raiser becomes unsymmetrical. On the basis of the work in reference 17, on unsymmetrically located holes, it would be expected that the departure from symmetry would result in even greater stresses at the initial crack tip; and it would seem that the initial crack, having a head start, should increase in length over the crack subsequently formed at the other side of the stress raiser. The experimental evidence is that while the initial crack continues to grow, but is still of very short length, the second crack forms and catches up to the first in length. Thereafter, the two increase in length at the same rate. These effects

2Q

suggest that residual compressive stresses and crack closure develop at the tip of the first crack which reduce its effectiveness as a stress raiser, whereas at the second-crack nucleus the residual stresses and crack closure are not as fully developed and allow the crack to grow more rapidly until it catches up to the first in length. Thereafter, conditions are about the same at each crack front, and the cracks increase in length at the same rate.

Nonpropagating Fatigue Cracks

In the case of nonpropagating fatigue cracks, the stress levels $\left(\text{and values of } K_N S_{net}\right)$ through necessity are very low. Hence, although ρ_e may vary with stress level, the values of ρ_e determined in references 13 and 14 from the minimum stress required for crack propagation are in the same stress range as nonpropagating cracks and should be applicable. From considerations of the stress at the tip of a crack, it appears that the manner in which nonpropagating fatigue cracks may be formed would depend upon the relative magnitude of the effective radius, the radius of the initial notch, and the influence of the material in determining the extent of crack closure during the compression portion of load cycles of negative R.

If the crack closed completely during unloading, the compression portion of the cycle would have little effect on crack propagation and the material at the tip of the crack could be considered to experience loading of essentially $R = 0$ rather than the applied negative R loading since the effect of the residual compressive stress had already been incorporated into the effective radius. On the other hand, if the crack remained open throughout the cycle, the tip loading could be considered to correspond to the applied negative R loading.

When a crack is formed, it is in a stress field which is the product of the net-section stress, the stress-concentration factor for the notch, and the stress-concentration factor for the crack itself. Under these combined effects the crack will grow out of the region of influence of the notch, after which its rate of propagation will depend on only the net-section stress and the stress-concentration factor for the crack. It is expected that the initial rate of propagation will always be higher because of the notch effect than it will be after the crack has advanced slightly, but as the crack gets larger, the rate will increase again because of the increase in the stress-concentration factor with the length of the crack. In the subsequent discussion it is assumed that the crack is outside the influence of the initial notch, but it is not long enough to affect the net-section stress. (For an internal crack, the length would be the tip-to-tip distance, which would include the length of the initial notch.)

There are essentially two ways by which nonpropagating cracks may be formed under constant-amplitude loading as shown in figure 3. If the effective radius of the fatigue crack is greater than that of the initial notch, a decrease in local stress will occur as indicated in figure 3(a), and a nonpropagating crack will be formed since the new effective peak stress will be less than the fatigue limit for the material. If the effective radius of the crack is less than that of the initial notch but the crack closes during the compression portion of the cycle, a nonpropagating crack may also be formed, for the effective range of stress at the tip of the crack would be decreased. For example, as shown in figure 3(b), where the crack closed during compression a loading of $R = -1$ would become an effective loading of $R_e = 0$ at the crack tip; and since the fatigue limit for loading with $R = 0$ is greater than that with $R = -1$, a nonpropagating crack could form even though the peak stress for the crack is higher than that for the initial notch (but less than the fatigue limit for loading with $R = 0$). For convenience in subsequent discussions, the two cases just described can also be depicted as shown in figure 4. In figure 4(a), which corresponds to figure 3(a), the value of S_{net} required to initiate a fatigue crack is seen to decrease with notch radius. Below $\rho_{notch} = \rho_e$ the value for crack initiation is less than the constant value for crack propagation, which depends only on effective stress concentration at the tip of the crack. Nonpropagating cracks thus may be formed in the shaded region. Note that as the radius approaches zero, a finite value of stress is required to initiate a fatigue crack in accord with the limiting case of equation (1).

L 4 2 9

Figure 4(b) corresponds to figure 3(b). Here, again, nonpropagating cracks may be formed within the shaded region even though now ρ_e may be less than ρ_{notch} because of the decrease in the severity of loading at the tip of the crack associated with the change from loading with $R_e = -1$ to that with $R_e = 0$. This case is similar to the model proposed by Coffin (ref. 10) in his qualitative explanation of the development of nonpropagating fatigue cracks.

ANALYSIS OF PUBLISHED DATA

Frost and Phillips Data in Reference 6

In order to make use of the published data in comparison with the concepts of the preceding section as summarized in figures 3 and 4 it is necessary to have a complete description of the configuration of the specimen and knowledge of the conditions of applied stress. Few of the investigations reported to date contain all of the required data. However, some contain sufficient data to be of interest, and among these is a paper by Frost and Phillips (ref. 6).

In reference 6 cylindrical specimens of mild steel (0.15 percent carbon), aluminum alloy (British Standard L.65 which is similar to 2024-T3), and nickel-chromium steel (British Standard En.26) were tested. Fatigue cracks were initiated in rotating beam specimens, and then the applied stress was reduced to determine the minimum stress at which such cracks would propagate. Since in these tests the cracked section was unsymmetrical, an equivalent stress was computed. The following comparison between the results obtained and vee-notched specimens with a notch 0.2 inch deep and of 0.002-inch radius is given:

L
4
2
9

Material	Fatigue limit of unnotched cracked specimens (equivalent computed stress), ksi	Fatigue limit of notched specimens, ksi
Mild steel	±12.3	±8.7
Nickel-chromium steel	±29.1	±10.1
Aluminum alloy . . .	±13.4	±5.6

From this comparison, it is concluded in reference 6 that fatigue cracks are not very efficient stress raisers. However, the results for the aluminum alloy are not in accord with the results of tests on sheet specimens presented in reference 14. In the latter case, the fatigue limit of specimens containing fatigue cracks was of the order of ±2.5 ksi. (The exact value depends upon K_N.) It is considered that this lower value is more representative for the following reasons:

The fatigue cracks in the tests in reference 6 on the aluminum alloy were introduced at a nominal stress level of ±38 ksi, and, of course, the corresponding local stress level increased as the crack grew. After the formation of the cracks the stress level was reduced to a nominal stress of approximately ±11 ksi to search out the fatigue limit by cycling for 10^7 cycles at progressively higher stress levels until fracture occurred. The initial sequence of high stress to low stress is of the type discussed in the preceding section and would introduce high residual compressive stresses, with resultant increase in the effective radius and corresponding increase in the fatigue limit. Such a test would not indicate the true fatigue limit of a crack, but rather it would strongly reflect the effect of previous stress history.

In the cited tests on sheet specimens (ref. 14), however, the cracks were introduced at stresses slightly above the fatigue limit; therefore, the specimens contained residual stresses associated only with the level of fatigue limit itself. For this aluminum alloy the effective radius was computed to be 0.003 inch, which reflects its effectiveness as a stress raiser in comparison with stress-free machined notches.

A further indication that high residual compressive stresses were present in reference 6 stems from the observation that no crack growth at all was observed at the lower stress levels prior to fracture of the specimens. (In addition, the lack of growth reported is not in accord with the findings of refs. 13 and 14 where crack growth prior to fracture was observed at all levels above the minimum stress level required to propagate the crack.) The result that no crack propagation was observed at the low stress level can be explained in the following manner: At the tip of the crack grown at the high stress level, high residual compressive stresses were present. At the lower stress level these residual stresses increased the magnitude of the stress required to propagate a fatigue crack over that for the constant-amplitude test. However, once this level for crack propagation was reached, the crack had to advance an amount so small that its growth was not observed as it grew out of the residual compressive stress field. The applied stress was now far in excess of that required to propagate a fatigue crack; in fact, it was so high that static failure occurred without sign of additional crack growth. It may be somewhat surprising that fracture did not occur at the high stress level and that it did occur at the lower level. This can be explained in that at the high stress level the material at the tip of the crack was plastically deformed; hence, not only high residual compressive stresses were introduced but the shape of the crack tip was altered by the plastic deformation. At the lower stress level once the crack left the high residual stress region it was a much more effective stress raiser, because of the absence of high residual stresses and also because of much less plastic deformation.

Another factor which may also contribute to the high value of the equivalent stress stated in reference 6 is the manner of computing this equivalent stress. Several assumptions concerning the distribution of stress had to be made, and if these were not quite correct, lower values for the equivalent stress would have been obtained. (See discussion by Heywood on p. 729 following ref. 6.)

It is believed that these same considerations apply as well to the mild steel and nickel-chromium steel results and that the equivalent stress fatigue limits are too high for these materials.

L
4
2
9

Frost Data in Reference 3

In reference 3 Frost describes tests in which fatigue cracks were grown at constant stress levels. Some of these cracks were of the non-propagating variety. The materials were a mild steel (0.15 percent carbon), a nickel-chromium steel (British Standard En.26), and an aluminum alloy (British Standard L.65). Both reversed direct stress and rotating bending fatigue tests were used. Only the results of the direct-stress tests of the aluminum alloy are discussed here as they are typical of the three materials.

L
4
2
9

The results of reference 3 are shown in figure 5. As can be seen, for notches of small radii an increase in fatigue limit is indicated. Such an increase is not consistent with the predictions of figure 4. In figure 5, the point representing the fatigue limit of a cracked specimen was taken from reference 6. This data point was discussed in the preceding section and was considered to be too high. In figure 5 the two points labeled A and B at small values of ρ are also considered to be high because of residual compressive stresses introduced in machining the small notches involved. Indeed, the X-ray work described in reference 18 indicates that compressive stresses of the order of 40 ksi can be developed in machining operations where the cutter is enclosed by the material of the job as would be the case in machining fine notches. In reference 3 there is no mention of any stress-relief anneal after machining. It is believed that, if the effects of the residual stresses associated with machining had been eliminated by annealing, the results would have been in accord with the predictions of figure 4.

Frost and Dugdale Data in Reference 4

In reference 4 Frost and Dugdale presented the results of constant-amplitude direct-stress fatigue tests on notched mild-steel plates, and both propagating and nonpropagating fatigue cracks were obtained. An important feature of this work is that the specimens were given a stress-relief anneal after machining. The results are shown in figure 6. In contrast to figure 5 (which is for an aluminum alloy, but the same type of results were obtained for mild steel), the curve does not rise for small values of ρ, in agreement with figure 4. It is believed that the anneal removed the residual stresses associated with machining, the stresses which influenced markedly the results in reference 3.

It is interesting to note that an explanation for nonpropagating cracks based on a flaw hypothesis is developed in reference 11. In this concept fatigue failure is associated with flaws inherent in the material. These flaws are of characteristic size, and as the notch radius decreases, the chance of having a flaw at the base of the notch also decreases; for notches of extremely small radii the fatigue strength could actually increase, which would be in accord with the trend of figure 5. However, since the results shown in this figure are believed to be affected by residual stresses, the explanation as presented in reference 11 is considered to be inapplicable, especially since no such trend is found in figure 6.

The data of reference 4 have been analyzed, and the results are also shown in figure 6. For this mild steel an effective radius of 0.003 inch was computed, with the assumption that ρ' and ρ_e could be taken as equal as for aluminum alloys. Note that figure 6 corresponds to the portion of figure 4(b) to the right of $\rho_{notch} = \rho_e$. The results indicate that cracks in mild steel are completely closed during compression and, therefore, give the type of behavior as predicted in figure 4(b).

L 4 2 9

The preceding review covers briefly a number of papers on the subject of nonpropagating cracks. Where analysis is possible, the data available indicate that the crack is completely closed during compression in line with the proposal of Coffin (ref. 10). However, none of the data is of the type where ρ_e is larger than the geometrical notch radius so that the predictions of figures 3(a) and 4(a) can be evaluated. In order to fill this gap, a number of tests on aluminum alloys have been made, and these tests are described in the following section.

PRESENT TESTS

General

Previous work (refs. 13 to 15) indicated that values of ρ_e for 2024-T3 and 7075-T6 aluminum alloys at levels of $K_N S_{net}$ in the region of the fatigue limit were 0.003 and 0.002 inch, respectively. In accord with the predictions of figure 4(a) it should be possible to develop nonpropagating cracks either at $R = 0$ or at $R = -1$ by initiating the cracks at notches of radii smaller than ρ_e, so that a decrease in K_N would occur upon formation of a crack. For properly chosen values of S_{net}, the resultant effective stress at the tip of the crack would then fall beneath the fatigue limit of the material, as in figure 3(a). Previous work with these aluminum alloys indicated that fatigue cracks did not close completely for loading with $R = -1$ at low stress levels; hence, the type of behavior based on change of effective R ratio with crack closure would not be expected. In order to check these predictions, a number of specimens with an initial radius of 0.001 inch and 0.005 inch were tested.

Specimens

The configuration of the approximately 0.08-inch-thick 2024-T3 and 7075-T6 sheet specimens is shown in figure 7. The longitudinal direction of the specimens corresponds to the rolling direction of the sheets involved. As shown in figure 7, the radius on one side of the stress raiser was 0.001 inch, and on the other side it was 0.005 inch. A 1/32-inch-diameter hole was drilled at the center of each specimen and a 1/32-inch-deep notch was cut in each side of the hole as shown. For notches of 0.005-inch radius a nylon thread impregnated with a fine valve-grinding compound was drawn repeatedly with a reciprocating motion across the edge to be cut. For notches of 0.001-inch radius, a 0.002-inch-diameter copper wire was used in place of the nylon thread. It is believed that the gentle abrasive action involved in forming the notches did not introduce any significant residual stresses. The theoretical stress-concentration factors associated with each of these notches is given in table I.

L
4
2
9

Tests

The specimens were tested in direct-stress fatigue machines operating at 1,800 cpm. Loadings at both $R = 0$ and $R = -1$ were used. The stress levels and associated values of $K_N S_{net}$ are given in table II. In general, the tests were continued to 10^8 cycles, but in a few cases the tests were conducted for fewer cycles to check the length of the cracks. Inasmuch as cracks were not visible on the surface of the specimens, it was necessary to remove the surface layers to examine the interior of the specimens, and this examination was usually facilitated by polishing and etching. Such a procedure, of course, eliminated the possibility of further testing so that only one observation per specimen could be made.

The values of S_{net} were selected so that the value of $K_N S_{net}$ for the 0.001-inch-radius notch was above the fatigue limit for the R ratio involved (obtained from ref. 19), whereas the level of $K_N S_{net}$ of the 0.005-inch-radius notch was below the fatigue limit. Hence, a crack should form at the 0.001-inch-radius notch but not at the 0.005-inch-radius notch. In order to obtain nonpropagating fatigue cracks the value of S_{net} was also such that the value of $K_N S_{net}$ for a crack outside the region of influence of the original notch would lie below the fatigue limit.

RESULTS AND DISCUSSION

The results of the tests are given in table II. In accord with the predictions, nonpropagating cracks were found in almost every case at the 0.001-inch-radius notch for loadings at both $R = 0$ and $R = -1$. Except for one case, a crack was formed whenever the value of $K_N S_{net}$ at the 0.001-inch-radius notch exceeded the fatigue limit of the material. The exception could easily be due to scatter in that the fatigue limit for that specimen (number 6) may have been greater than average. Nonpropagating cracks were formed in all cases where the value of $K_N S_{net}$ for the fatigue crack was close to the fatigue limit of the material. Actually, nonpropagating cracks should be found only for values of $K_N S_{net}$ below the fatigue limit; but in view of the uncertainty of this latter value, the agreement is considered to be satisfactory. In no case did a crack form at the 0.005-inch-radius notch, in accord with the predictions, except where the value of $K_N S_{net}$ for this notch was above the fatigue limit. Typical photomicrographs are shown in figure 8.

L
4
2
9

From the tests terminated at fewer than 10^8 cycles, it was found that small cracks were present after 10^7 cycles and that cracks with a length about equal to those found at 10^8 cycles were present at 3×10^7 cycles. The fact that the length was about the same at 10^8 cycles as at 3×10^7 cycles is a further indication that the cracks were of the nonpropagating variety. A factor which may account for the difference in behavior between these aluminum alloys (cracks do not close) and mild steel (cracks close) is that the yield-fatigue ratio is about 3 for the aluminum alloys and only 1.5 for mild steel. From figure 1(a) it is seen that, where the resultant amplitude is small compared to the yield limit, the cracks do not close; but in figure 1(c), where the resultant amplitude is large compared to the yield limit, the cracks do close.

CONCLUDING REMARKS

The results obtained in the present investigation on aluminum alloys taken together with results obtained previously on mild steel indicate two ways by which nonpropagating cracks may be formed under constant-amplitude loading in specimens initially free of residual stresses. In the first case, a crack can form because the crack is not as effective a stress raiser as the initial notch; in the second case, the crack may close during the compression part of a test with $R = -1$ (where R is the ratio of minimum stress to maximum stress), thereby effectively transforming the local loading at the crack to loading at $R = 0$ with which a greater stress is required to propagate a fatigue crack. These same considerations could apply regardless of the ratio of R involved.

In a previous investigation it was concluded that a critical value of theoretical stress-concentration factor K_T was associated with nonpropagating cracks. The present results refute this contention, for the critical parameter is not K_T but rather the combined effects of the theoretical stress-concentration factor corrected for size effect K_N, the effective radius of a fatigue crack ρ_e, and the instantaneous net-section stress S_{net}.

L
4
2
9

It is further concluded that the stress required to propagate a crack may be increased if high residual compressive stresses due to prior loading or machining are present.

In the present work and in previous work it has been shown that the effectiveness of a fatigue crack in reducing the strength of a specimen depends both upon the length of the crack and upon the configuration of the specimen. The effective radius of a fatigue crack depends upon the stress history of the specimen in that the compressive residual stresses present at the tip of the crack influence the value of the effective radius. The present results do not indicate the magnitude of increase of the effective radius with stress level, but the change may be small in that results of prior static tensile tests on specimens containing fatigue cracks grown at various stress levels did not indicate a significant variation in ρ_e. For constant-stress-level crack propagation, results can be correlated with a single value for ρ_e, but where the stress level is varied additional experimental work is needed.

Finally, the results indicate that a method previously developed in NACA Technical Notes 3816 and 4394 and NASA Technical Note D-52 in connection with the propagation of fatigue cracks can be extended without modification to account for nonpropagating fatigue cracks in aluminum alloys, but additional considerations involving crack closure are required to account for this phenomenon in mild steel.

Langley Research Center,
National Aeronautics and Space Administration,
Langley Field, Va., October 13, 1959.

REFERENCES

1. Fenner, A. J., Owen, N. B., and Phillips, C. E.: The Fatigue Crack as a Stress-Raiser. Engineering, vol. 171, no. 4452, May 25, 1951, pp. 637-638.

2. Frost, N. E.: Crack Formation and Stress Concentration Effects in Direct Stress Fatigue. The Engineer, vol. 200, no. 5201, Sept. 30, 1955, pp. 464-467; no. 5202, Oct. 7, 1955, pp. 501-503.

3. Frost, N. E.: Non-Propagating Cracks in Vee-Notched Specimens Subject to Fatigue Loading. Aero. Quarterly, vol. VIII, pt. 1, Feb. 1957, pp. 1-20.

4. Frost, N. E., and Dugdale, D. S.: Fatigue Tests on Notched Mild Steel Plates With Measurements of Fatigue Cracks. Jour. Mech. Phys. Solids, vol. 5, no. 3, 1957, pp. 182-192.

5. Phillips, C. E.: Fatigue Cracks as Stress Raisers and Their Response to Cyclic Loading. Fatigue in Aircraft Structures, Alfred M. Freudenthal, ed., Academic Press, Inc. (New York), 1956, pp. 104-125.

6. Frost, N. E., and Phillips, C. E.: The Fatigue Strength of Specimens Containing Cracks. Proc. Inst. Mech. Eng. (London), vol. 170, no. 21, 1956, pp. 713-725; Discussion, pp. 726-738.

7. Frost, N. E., and Dugdale, D. S.: The Propagation of Fatigue Cracks in Sheet Specimens. Jour. Mech. Phys. Solids, vol. 6, no. 2, 1958, pp. 92-110.

8. Frost, N. E., and Phillips, C. E.: Studies in the Formation and Propagation of Cracks in Fatigue Specimens. Proc. Int. Conf. on Fatigue of Metals (London and New York), Inst. Mech. Eng. and A.S.M.E., 1956, pp. 520-526.

9. Frost, N. E., and Phillips, C. E.: Some Observations on the Spread of Fatigue Cracks. Proc. Royal Soc. (London), ser. A, vol. 242, no. 1229, Oct. 29, 1957, pp. 216-222.

10. Coffin, L. F., Jr.: A Mechanism for Nonpropagating Fatigue Cracks. Proc. ASTM, vol. 58, 1958, pp. 570-575.

11. Harris, W. J.: "Size" Effects and Their Possible Significance for "Non-Propagating" Cracks in Metal Fatigue. Metallurgia, vol. 57, no. 342, Apr. 1958, pp. 193-197.

L
4
2
9

12. McEvily, Arthur J., Jr., Illg, Walter, and Hardrath, Herbert F.: Static Strength of Aluminum-Alloy Specimens Containing Fatigue Cracks. NACA TN 3816, 1956.

13. McEvily, Arthur J., Jr., and Illg, Walter: The Rate of Fatigue-Crack Propagation in Two Aluminum Alloys. NACA TN 4394, 1958.

14. Illg, Walter, and McEvily, Arthur J., Jr.: The Rate of Fatigue-Crack Propagation for Two Aluminum Alloys Under Completely Reversed Loading. NASA TN D-52, 1959.

L
4
2
9

15. Neuber, Heinz: Theory of Notch Stresses: Principles for Exact Stress Calculation. J. W. Edwards (Ann Arbor, Mich.), 1946.

16. Howland, R. C. J.: On the Stresses in the Neighbourhood of a Circular Hole in a Strip Under Tension. Phil. Trans. Roy. Soc. (London), sec. A, vol. 229, no. 671, Jan. 6, 1930, pp. 49-86.

17. Sjöström, S.: On the Stresses at the Edge of an Eccentrically Located Circular Hole in a Strip Under Tension. Rep. No. 36, Aero. Res. Inst. of Sweden (Stockholm), 1950.

18. Frommer, Leopold, and Lloyd, E. H.: The Measurement of Residual Stresses in Metals by the X-Ray Back-Reflection Method, With Special Reference to Industrial Components in Aluminum Alloys. Jour. Inst. Metals (London), vol. LXX, 1944, pp. 91-124.

19. Grover, H. J., Hyler, W. S., Kuhn, Paul, Landers, Charles B., and Howell, F. M.: Axial-Load Fatigue Properties of 24S-T and 75S-T Aluminum Alloy as Determined in Several Laboratories. NACA Rep. 1190, 1954. (Supersedes NACA TN 2928.)

TABLE I

DETAILS OF SPECIMEN GEOMETRY

Specimen	Aluminum alloy	ρ_{notch}, in.		ρ_e, in.	l, in.	Values of K_T for -			Values of K_N for -		
		Left	Right			0.001-inch-radius notch	Crack	0.005-inch-radius notch	0.001-inch-radius notch	Crack	0.005-inch-radius notch
1	2024-T3	0.001	0.005	0.003	0.079	10.93	6.74	5.44	4.64	3.87	3.50
2	2024-T3	.001	.005	.003	.089	11.40	7.00	5.65	4.81	4.00	3.62
3	2024-T3	.001	.005	.003	.071	10.65	6.58	5.31	4.53	3.79	3.43
4	2024-T3	.001	.005	.003	.100	11.63	7.14	6.45	4.90	4.07	3.68
5	2024-T3	.001	.005	.003	.081	11.05	6.80	5.50	4.68	3.90	3.54
6	7075-T6	.001	.005	.002	.067	10.49	7.70	5.25	4.93	4.45	3.60
7	7075-T6	.001	.005	.002	.091	11.37	8.34	5.64	5.30	4.67	3.84
8	7075-T6	.001	.005	.002	.159	12.55	9.20	6.17	5.79	5.10	4.17

TABLE II

RESULTS OF CRACK-PROPAGATION TESTS

Specimen	R	S_{net}, ksi	Values of $K_N S_{net}$, ksi, for -			Fatigue limit, ksi	Number of cycles	Remarks
			0.001-inch-radius notch	Crack	0.005-inch-radius notch			
1	0	7.83	36.3	30.6	27.4	30	10^8	Nonpropagating crack formed at 0.001-inch-radius notch
2	0	9.10	43.5	36.2	32.8	30	2×10^6	Specimen failed (propagating cracks formed at both notches)
3	0	7.93	35.9	30.0	27.2	30	10^7	Small cracks formed at at 0.001-inch-radius notch
4	0	7.38	36.2	30.0	27.2	30	3×10^7	Nonpropagating crack formed at 0.001-inch-radius notch
5	-1	4.27	19.9	16.6	15.0	18	10^8	Nonpropagating crack formed at 0.001-inch-radius notch
6	0	6.40	31.5	28.5	23.0	30	10^8	No crack
7	0	6.45	34.2	30.2	24.8	30	10^8	Nonpropagating crack formed at 0.001-inch-radius notch
8	-1	3.50	20.2	17.8	14.6	18	10^8	Nonpropagating crack formed at 0.001-inch-radius notch

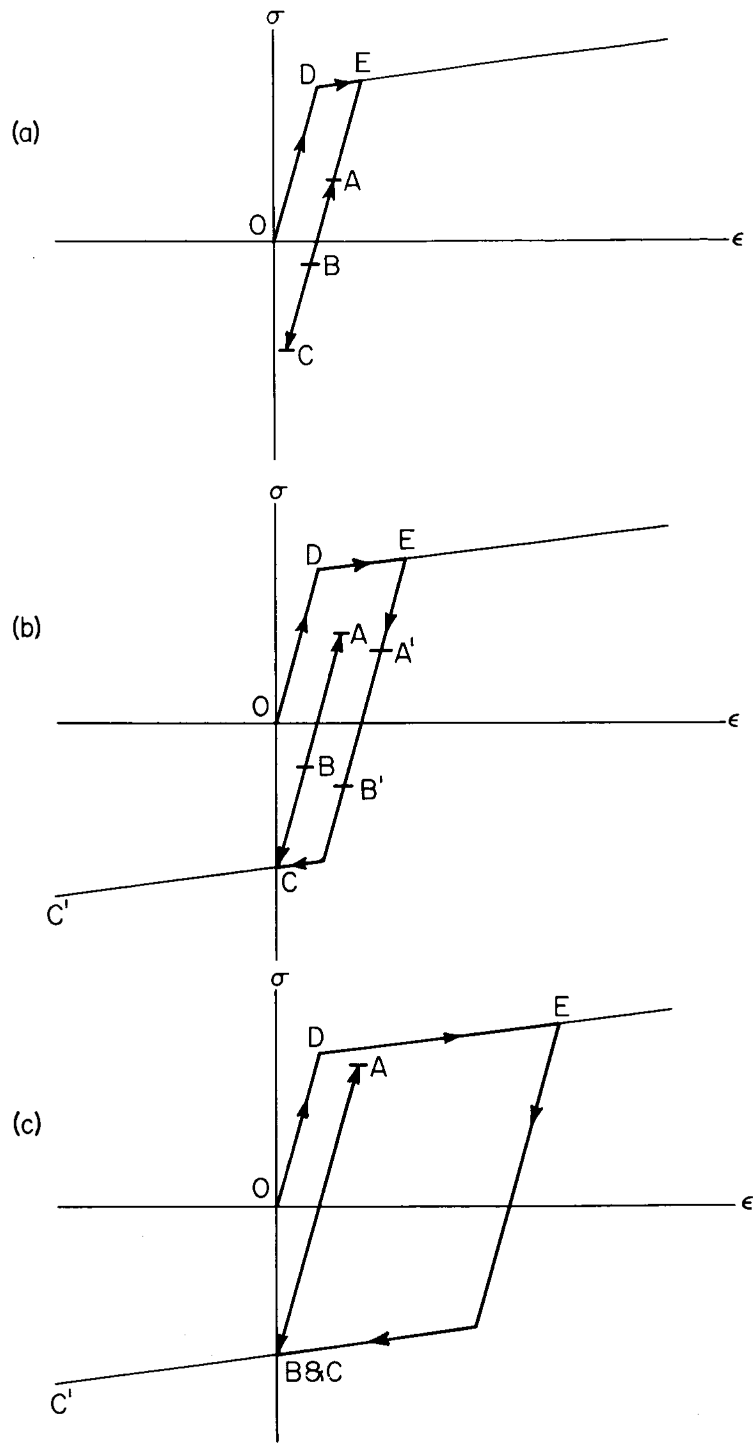

Figure 1.- Idealized stress-strain behavior at the tip of a fatigue crack for three levels of nominal stress.

L-429

L-429

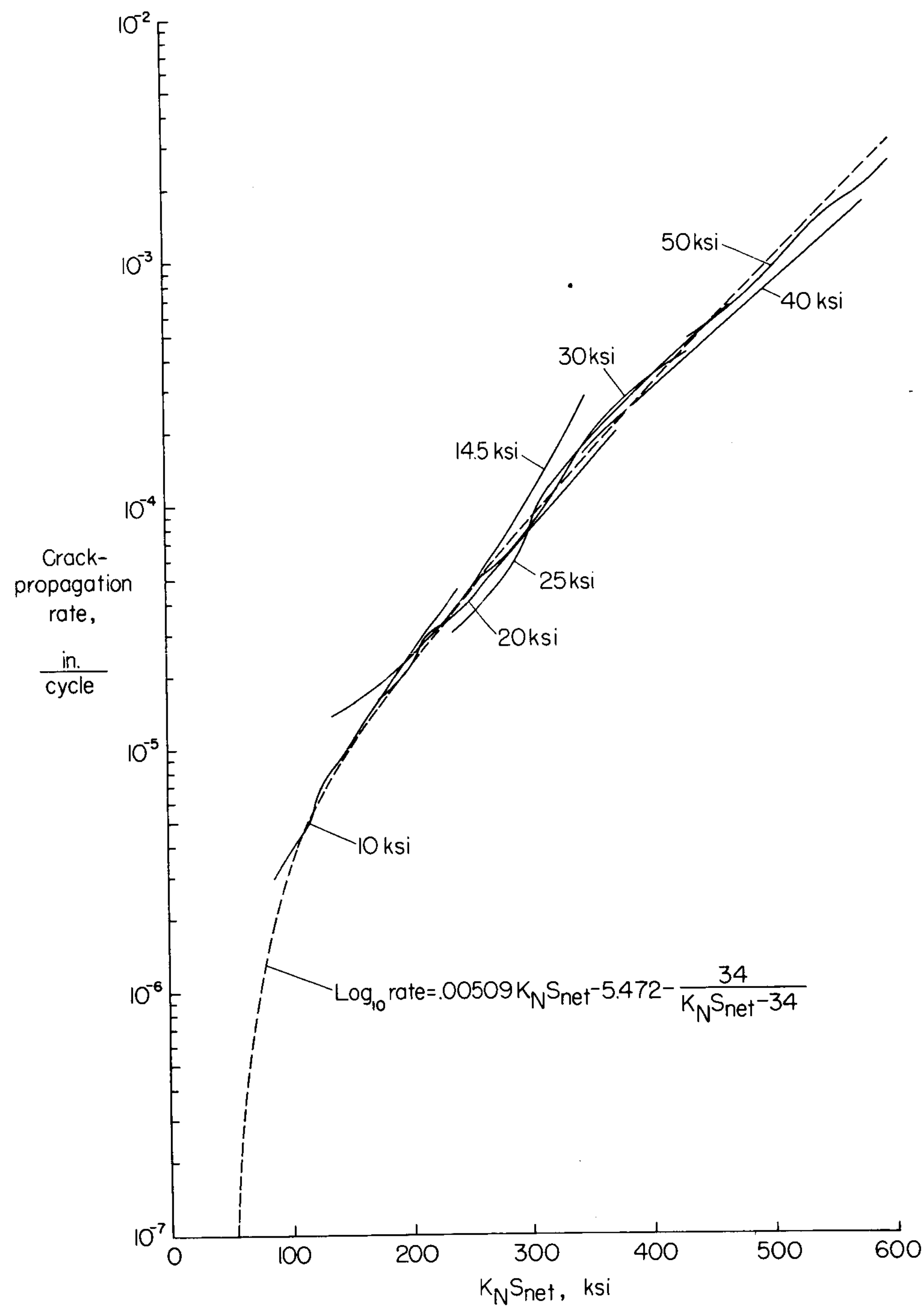

Figure 2.- Rates of fatigue-crack propagation in 12-inch-wide 7075-T6 aluminum-alloy sheet specimens. Stress values on curves indicate initial nominal cyclic stress (ref. 13).

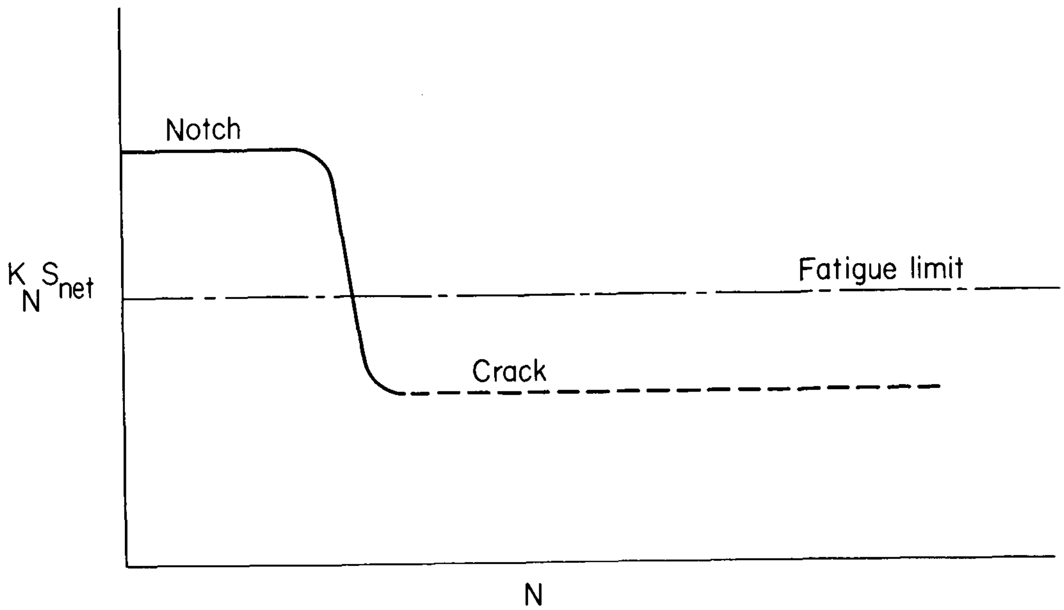

(a) Case I where $\rho_{crack} > \rho_{notch}$ and crack does not close.

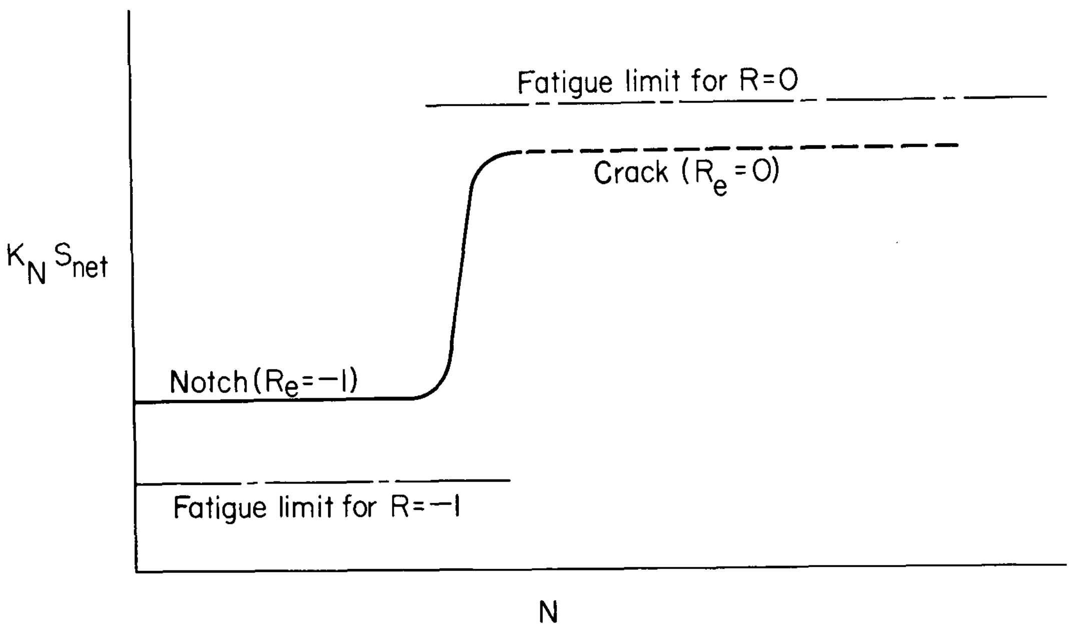

(b) Case II where $\rho_{crack} < \rho_{notch}$, R = -1, and crack closes during compression.

Figure 3.- Two ways of forming nonpropagating cracks in notched specimens.

L-429

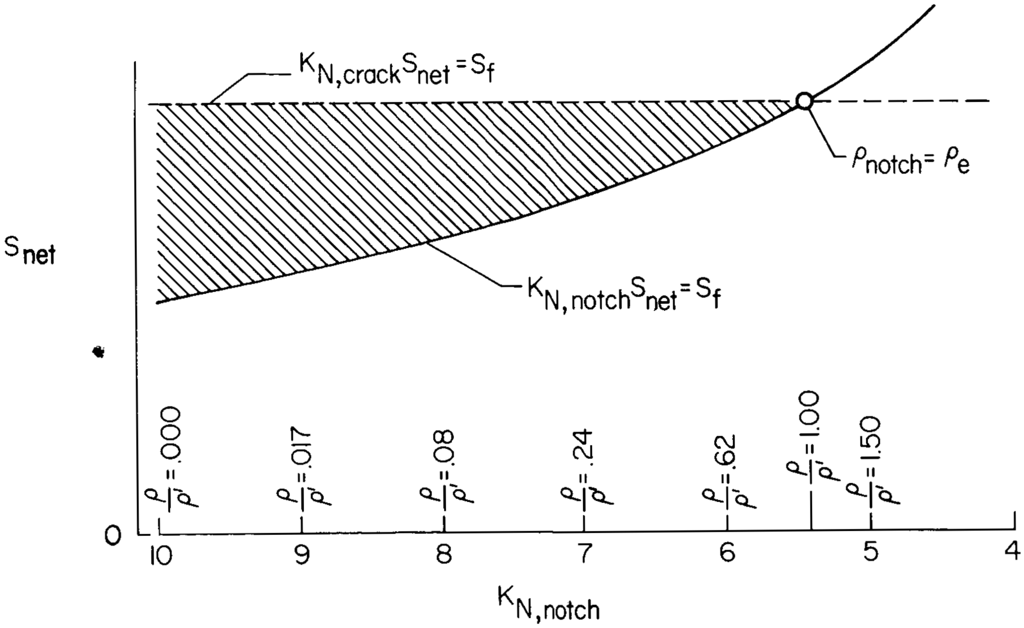

(a) Case I with no crack closure.

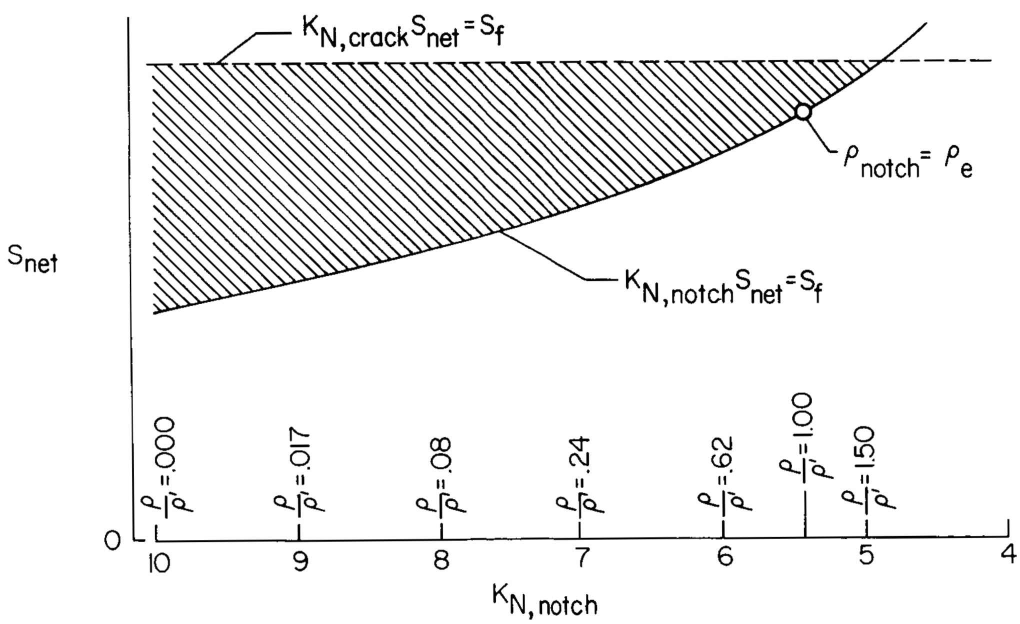

(b) Case II where crack closes during compression.

Figure 4.- Relations between net stress and notch severity for initiation and propagation of fatigue cracks in constant-load cyclic tests. Nonpropagating fatigue cracks occur in crosshatched region.

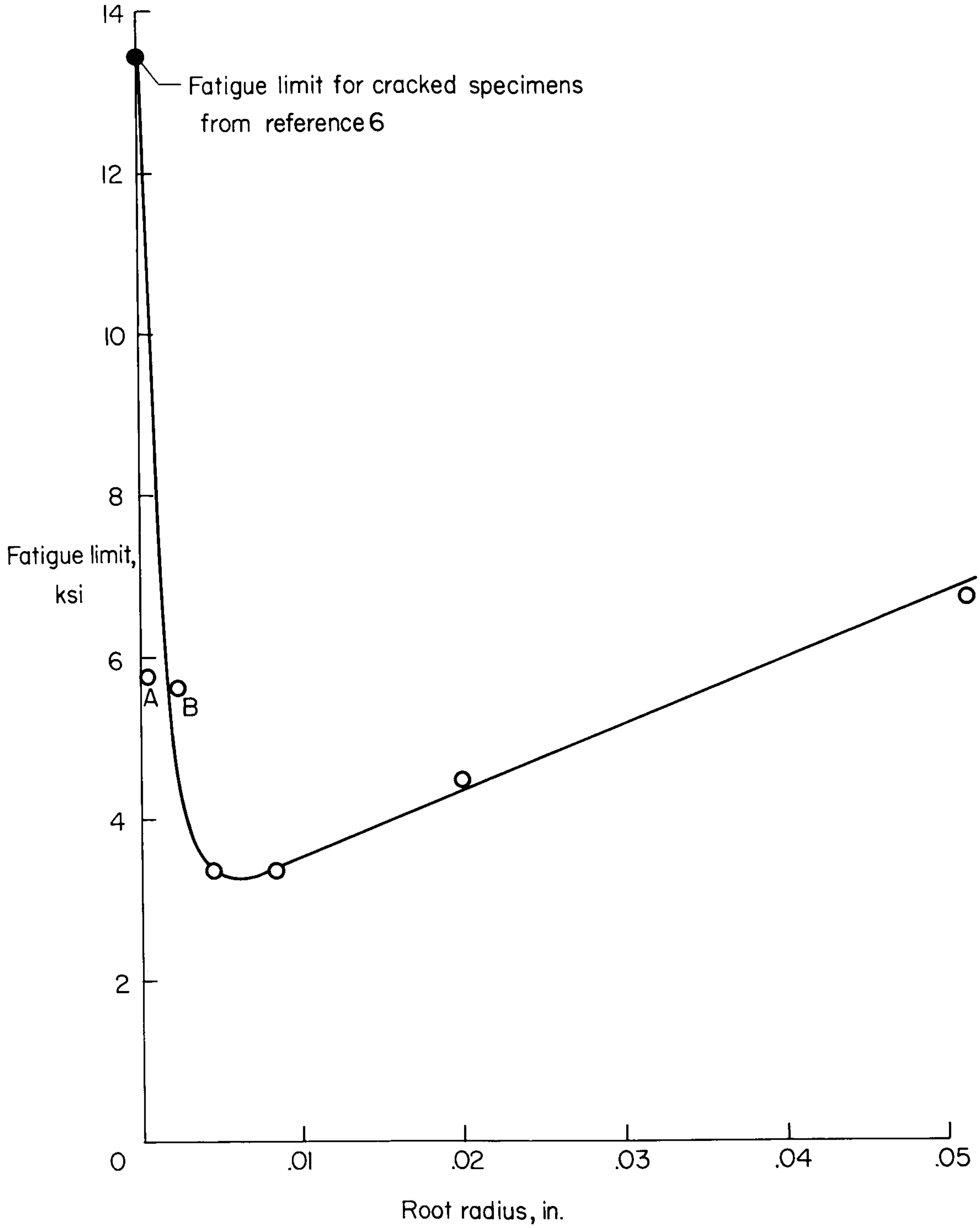

Figure 5.- Data from reference 3 on initiation and propagation of fatigue cracks in notched aluminum-alloy specimens.

L-429

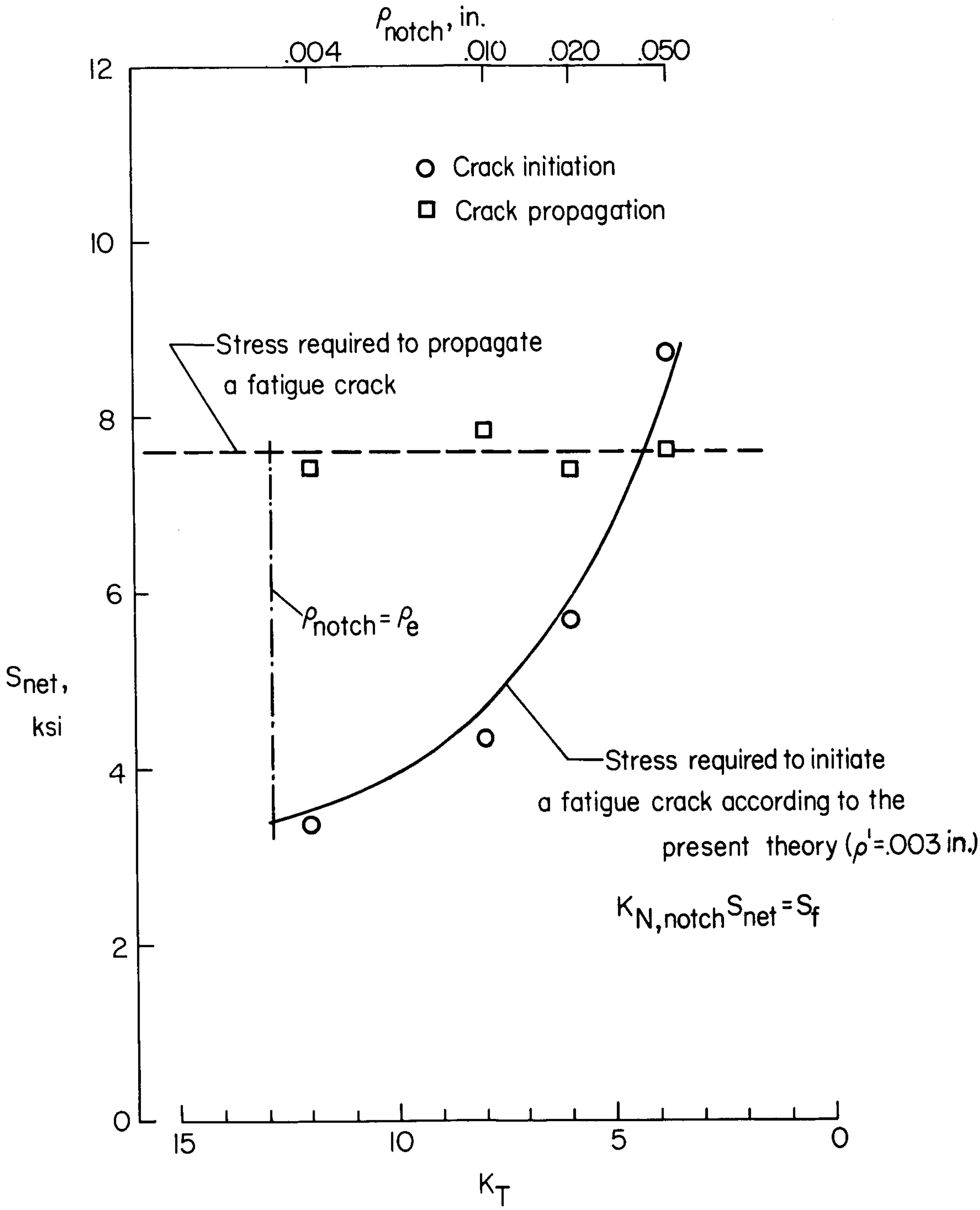

Figure 6.- Comparison between direct-stress test data of reference 4 on mild-steel sheet and present calculations. R = -1.

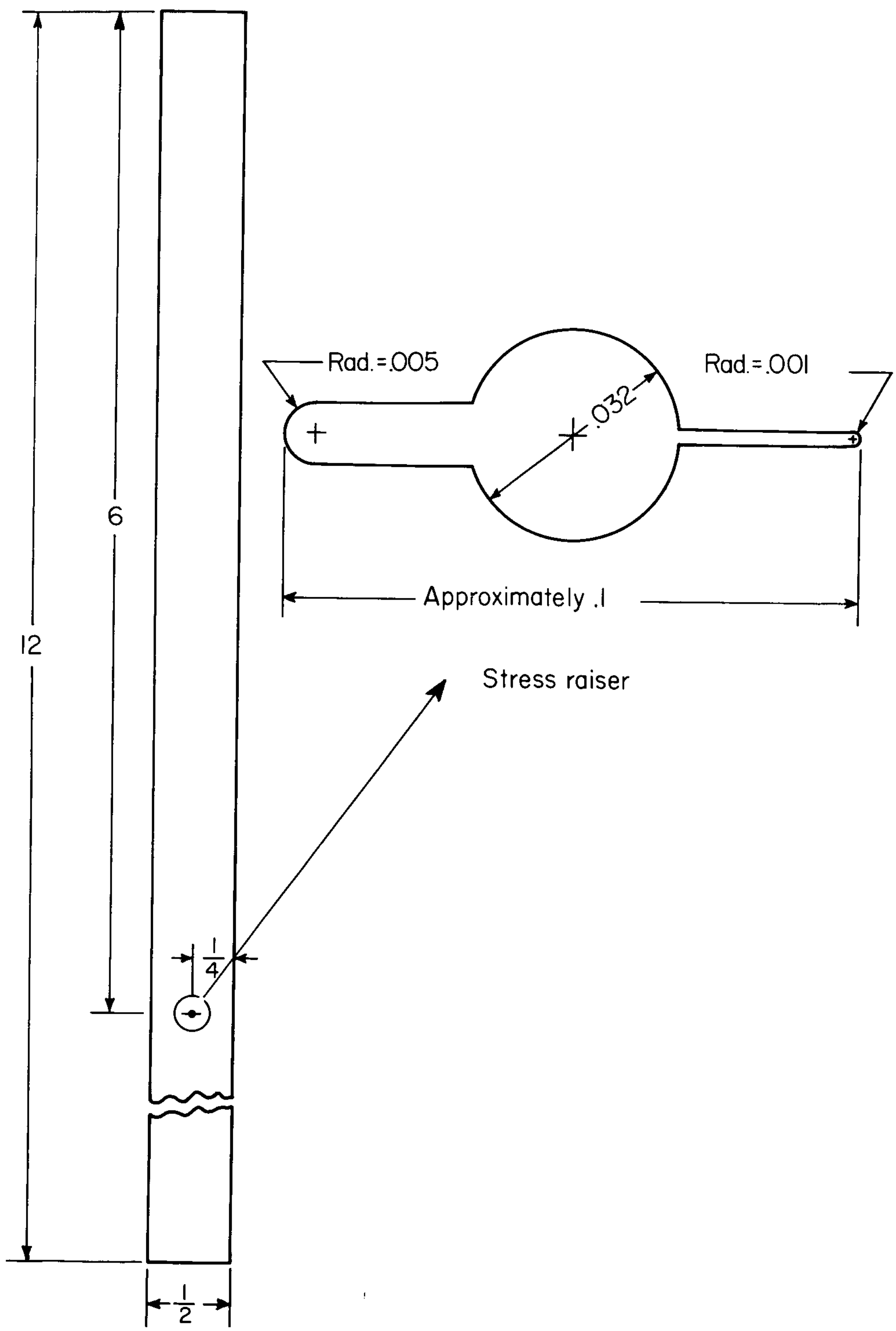

L-429

Figure 7.- Specimen configuration. All dimensions are in inches.

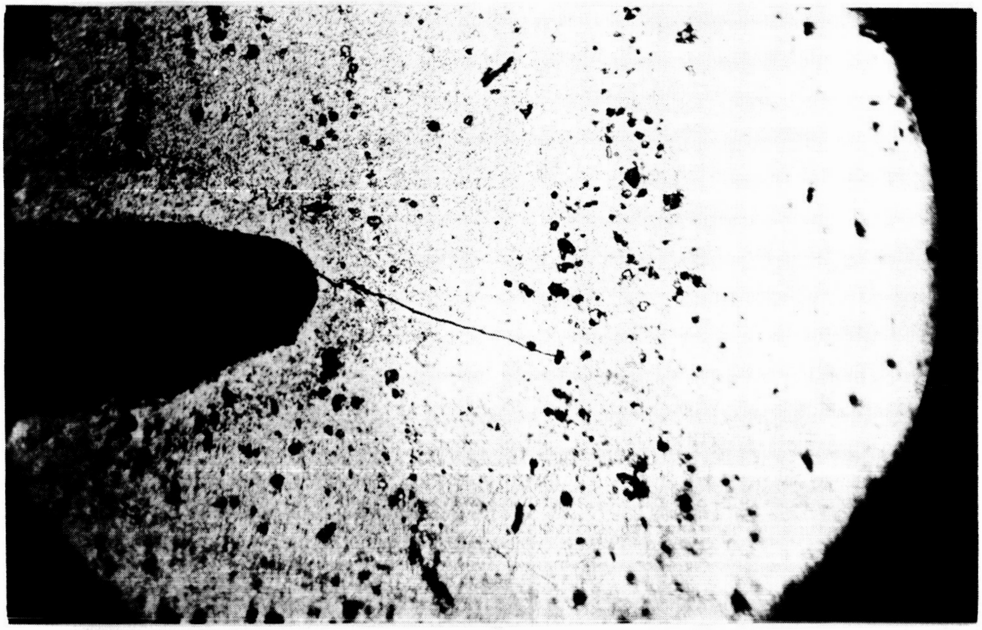

(a) 2024-T3 aluminum alloy.

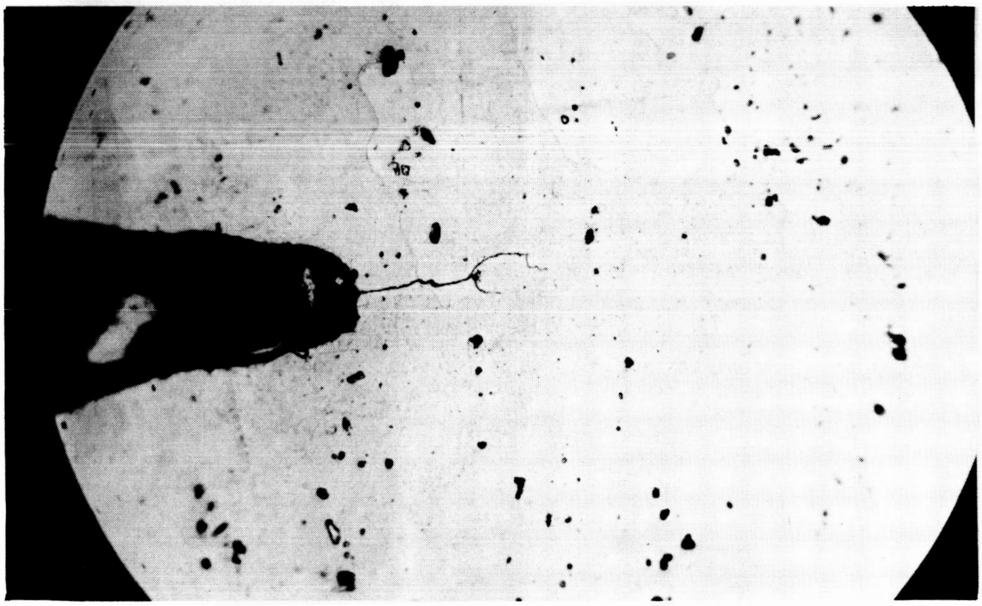

(b) 7075-T6 aluminum alloy. L-59-6100

Figure 8.- Photomicrographs of typical nonpropagating cracks at a 0.001-inch-radius notch in two aluminum alloys. (×440)